DOI: 10.1002/ejic.200700950

Cobalt(III) Complexes of a Tripodal Ligand Containing Three Imidazole Groups: Properties and Structures of Racemic and Optically Active Species

Hirofumi Nakamura,[a] Megumi Fujii,[a] Yukinari Sunatsuki,[a] Masaaki Kojima,*[a] and Naohide Matsumoto[b]

Keywords: Cobalt / Crystal structure / Chiral resolution / Schiff bases / N ligands / Tripodal ligands

The complex $[Co(H_3L)](ClO_4)_3{\cdot}H_2O$ (**1**), where H_3L {tris[2-(4-imidazoylmethylideneamino)ethyl]amine} is a tripodal ligand obtained by condensation of tris(2-aminoethyl)amine and 4-formylimidazole in a 1:3 molar ratio, was synthesized and optically resolved by fractional crystallization of the diastereomeric salt with $[Sb_2\{(R,R)\text{-tart}\}_2]^{2-}$ [(*R*,*R*)-tart = (2*R*,3*R*)-tartrate(4–) ion]. From the less soluble part, Λ-$[Co(H_2L)][Sb_2\{(R,R)\text{-tart}\}_2]{\cdot}4H_2O$ (**2**) was isolated. Starting from **2**, two optically active complexes, Λ-$[Co(H_3L)](ClO_4)_3{\cdot}1.5H_2O$ (Λ-**1**) and Λ-[Co(L)] (Λ-**3**), were obtained. The crystal structures of these complexes are compared with those of the racemic structures. Λ-**1** shows an unusually strong circular dichroism (λ = 488 nm, $\Delta\varepsilon$ = –7.74 $M^{-1}cm^{-1}$) in the first d–d absorption band region. The effects of deprotonation–reprotonation of the uncoordinated imidazole NH groups of Λ-$[Co(H_3L)]^{3+}$ on the UV/Vis and CD spectra and on the cyclic voltammograms were studied in methanol. Although the deprotonation–reprotonation reactions are reversible, the redox couple for the completely deprotonated species $[Co^{III/II}(L)]^{0/-}$ is not observed.

Introduction

Racemic crystals (racemic compounds), where each crystal contains the enantiomers in a 1:1 ratio, are usually formed when a racemate aggregates and condenses. This fact indicates that heterochiral interaction is usually stronger than homochiral interaction. Statistically, only 5–10% of racemates form conglomerates (racemic mixtures)[1] where each crystal contains only one enantiomer and the solid racemate is simply a 1:1 mechanical mixture of individual crystals each consisting of a single enantiomer.

Recently, we reported the synthesis, structure, and magnetic properties of the spin-crossover iron(II) complex $[Fe^{II}(H_3L)](BF_4)_2{\cdot}3H_2O$ of the tripodal ligand tris[2-(4-imidazoylmethylideneamino)ethyl]amine (H_3L; Figure 1a), which contains three imidazole groups.[2] The complex is chiral with either a Δ (clockwise) or a Λ (anticlockwise) configuration due to the screw coordination arrangement of the achiral tripodal ligand around the Fe^{II} ion (Figure 1b). Adjacent complex cations with the same absolute configuration are connected in a tail-to-tail fashion by N–H···O(H_2O)···H–N hydrogen bonds in the crystal to form a puckered 2D sheet structure based on a hexanuclear unit (Figure 1c).[2] Furthermore, sheets with the same chirality are stacked to form a chiral crystal, thus indicating that conglomerate crystallization has occurred during the crystallization process.[2] The perchlorate $\{[Fe^{II}(H_3L)](ClO_4)_2{\cdot}3H_2O\}$[3a] and nitrate $\{[Fe^{II}(H_3L)](NO_3)_2{\cdot}3H_2O\}$[3b] analogs also undergo conglomerate crystallization, whereas the chloride $\{[Fe^{II}(H_3L)]Cl_2{\cdot}6H_2O\}$[3c] and thiocyanate $\{[Fe^{II}(H_3L)](SCN)_2\}$[3c] salts undergo heterochiral crystallization to form racemic crystals. A comparison of the crystal structures of the homochiral and heterochiral complexes would be helpful for understanding the mechanism of chiral discrimination, therefore we decided to study the stereochemically inert cobalt(III) complexes. None of the complexes $[Co(H_3L)](ClO_4)_3{\cdot}H_2O$ (**1**), $[Co(H_3L)](PF_6)_3{\cdot}2H_2O$, or $[Co(L)]{\cdot}2.5H_2O$ (**3**) undergoes conglomerate crystallization, and their deprotonation is associated with the uncoordinated imidazole moieties. We resolved $[Co(H_2L)]^{2+}$ by fractional crystallization of the diastereomeric salt with $[Sb_2\{(R,R)\text{-tart}\}_2]^{2-}$ [(*R*,*R*)-tart = (2*R*,3*R*)-tartrate(4–) ion] and obtained Λ-$[Co(H_3L)]^{3+}$ from the less soluble diastereomer. Herein we compare the crystal structures of the perchlorate salts Λ-$[Co(H_3L)](ClO_4)_3{\cdot}1.5H_2O$ (Λ-**1**), which is optically active, and *rac*-$[Co(H_3L)](ClO_4)_3{\cdot}H_2O$ (**1**), which is racemic, and the crystal structures of the deprotonated species Λ-[Co(L)] (Λ-**3**) and *rac*-$[Co(L)]{\cdot}2.5H_2O$ (**3**). We also report the properties of Λ-$[Co(H_3L)](ClO_4)_3{\cdot}1.5H_2O$, with emphasis being placed on the effect of deprotonation on the UV/Vis and CD (circular dichroism) spectra and on the cyclic voltammograms.

[a] Department of Chemistry, Faculty of Science, Okayama University,
Tsushima-naka 3-1-1, Okayama 700-8530, Japan
Fax: +81-86-251-7842
E-mail: kojima@cc.okayama-u.ac.jp
[b] Department of Chemistry, Faculty of Science, Kumamoto University,
Kurokami 2-39-1, Kumamoto 860-8555, Japan

Supporting information for this article is available on the WWW under http://www.eurjic.org or from the author.

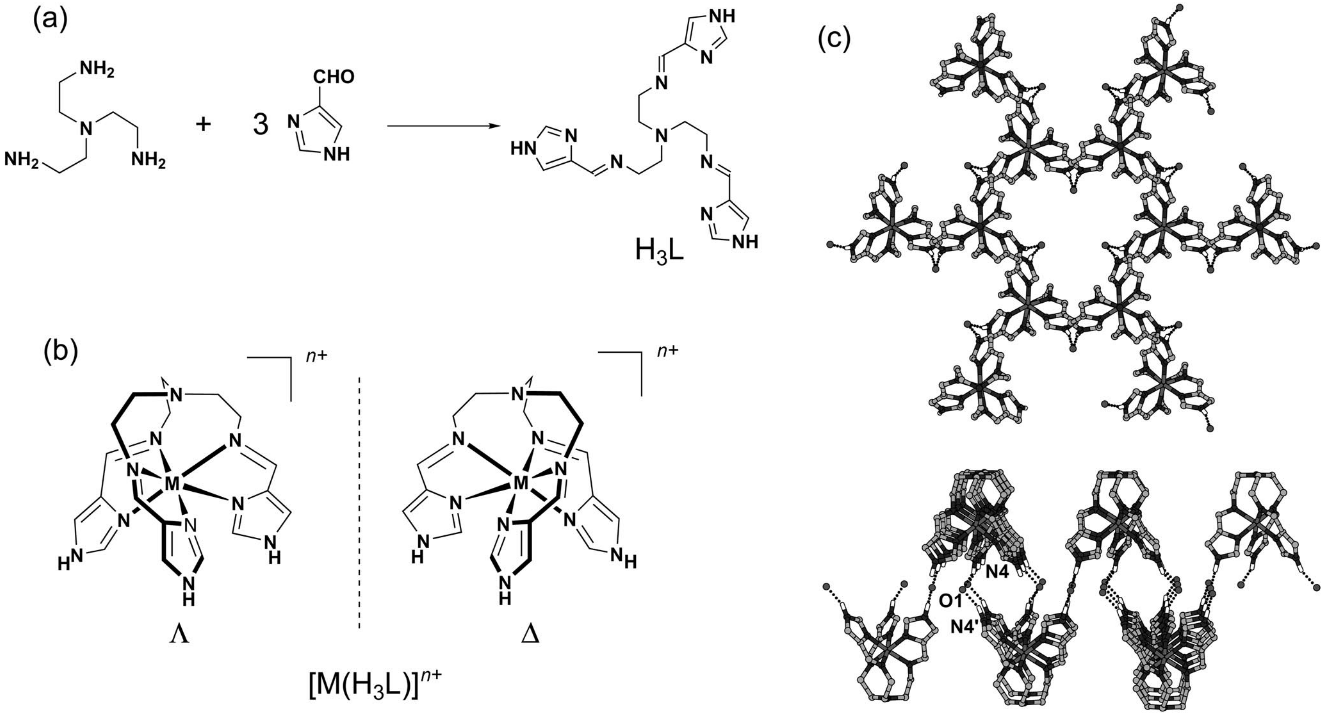

Figure 1. (a) Synthesis of the tripodal ligand H_3L. (b) Δ and Λ configurations of $[M(H_3L)]^{n+}$. (c) Top (top) and side views (bottom) of the crystal structure of $[Fe^{II}(H_3L)](BF_4)_2\cdot 3H_2O$ showing a 2D sheet formed by intermolecular hydrogen bonds through water molecules. Each complex cation has a crystallographic threefold axis. The counteranions have been omitted for clarity.

Results and Discussion

Synthesis, Characterization, and Properties

The tripodal ligand H_3L[4] was prepared by a condensation reaction between tris(2-aminoethyl)amine and 4-formylimidazole in a 1:3 molar ratio in methanol (Figure 1a). The ligand was not isolated, and a solution containing the ligand was allowed to react with *trans*-$[CoCl_2(py)_4]Cl$[5] (1:1) to yield $[Co(H_3L)]^{3+}$, which was isolated as the perchlorate complex $[Co(H_3L)](ClO_4)_3\cdot H_2O$ (**1**). The uncoordinated NH groups of the imidazole moieties of **1** can be deprotonated with a base, and the fully deprotonated form of the complex, $[Co(L)]\cdot 2.5H_2O$ (**3**), was obtained by addition of excess base.[4]

Although H_3L is achiral, $[Co(H_3L)]^{3+}$ and its deprotonated forms are chiral due to the spiral coordination arrangement of the tripodal ligand around the Co^{III} ion (Figure 1b). Optical resolution was carried out by repeated recrystallization of the diastereomeric salt of $[Co(H_2L)]^{2+}$ with $[Sb_2\{(R,R)\text{-tart}\}_2]^{2-}$ until the CD intensity became constant. One of the uncoordinated NH groups of the imidazole moieties of $[Co(H_3L)]^{3+}$ had to be deprotonated to increase the solubility difference between the diastereomeric salts. We isolated the diastereomeric salt $\{(-)_{487}\}_{CD}$-$[Co(H_2L)][Sb_2\{(R,R)\text{-tart}\}_2]\cdot 4H_2O$ (**2**), which has a negative CD band at 487 nm, from the less soluble part. The resolution was unsuccessful when $[Co(H_3L)]^{3+}$ was allowed to react with $[Sb_2\{(R,R)\text{-tart}\}_2]^{2-}$ without the addition of a base. The absolute configuration about the Co ion of the $\{(-)_{487}\}_{CD}$ salt was determined to be Λ by X-ray crystallography. All our efforts to isolate the more soluble diastereomeric salt involving the isomer Δ-$[Co(H_2L)]$-$[Sb_2\{(R,R)\text{-tart}\}_2]$ were unsuccessful. We subsequently prepared the optically active complexes Λ-$[Co(H_3L)](ClO_4)_3\cdot 1.5H_2O$ (Λ-**1**) and Λ-$[Co(L)]$ (Λ-**3**) from **2**.

Figure 2 shows the UV/Vis and CD spectra of Λ-$[Co(H_3L)](ClO_4)_3\cdot 1.5H_2O$ (Λ-**1**; $3d^6$, t_{2g}^6) in dmso. The data are listed in Table 1 together with those of Λ-$[Co(H_2L)][Sb_2\{(R,R)\text{-tart}\}_2]\cdot 4H_2O$ (**2**), Λ-$[Co(L)]$ (Λ-**3**), and H_3L. The first d–d absorption band $[^1T_{1g} \leftarrow {}^1A_{1g}\ (O_h)]$ of Λ-**1** is observed as a shoulder (λ = 480 nm, ε = 260 $M^{-1}cm^{-1}$) of an intense imine π–π* transition ($\lambda \approx$ 320 nm, ε = 5000 $M^{-1}cm^{-1}$), which obscures the weak second d–d absorption band $[^1T_{2g} \leftarrow {}^1A_{1g}\ (O_h)]$.[6] The intense band at 273 nm is due mainly to the imidazole moiety. The complex Λ-$[Co(H_3L)](ClO_4)_3\cdot 1.5H_2O$ (Λ-**1**) obtained from the less soluble diastereomeric salt **2** exhibits a negative CD band in the first d–d absorption band region (λ = 488 nm, $\Delta\varepsilon$ = –7.74 $M^{-1}cm^{-1}$).

The CD spectra of tris(chelate) complexes such as $[Co(en)_3]^{3+}$ (en = ethylenediamine) have been studied extensively,[7] and it should be noted that Λ-$[Co(en)_3]^{3+}$ shows a completely different CD pattern in this region from that of Λ-**1**. Thus, a main positive (λ = 490 nm, $\Delta\varepsilon$ = +1.89 $M^{-1}cm^{-1}$) and a weak negative CD band (λ = 429 nm, $\Delta\varepsilon$ = –0.12 $M^{-1}cm^{-1}$) are observed in the first d–d absorption band region (λ = 467 nm, ε = 93 $M^{-1}cm^{-1}$). The structure of **1** more closely resembles that of $[Co(sen)]^{3+}$

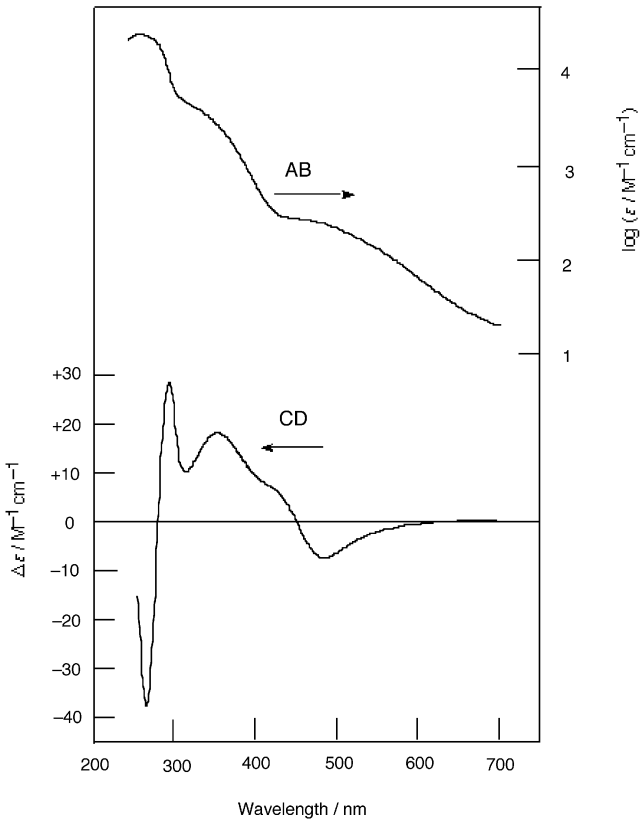

Figure 2. UV/Vis and CD spectra of Λ-$[Co(H_3L)](ClO_4)_3$·$1.5H_2O$ (Λ-**1**) in dmso.

Table 1. UV/Vis and CD spectroscopic data for Λ-$[Co(H_3L)](ClO_4)_3$·$1.5H_2O$ (Λ-**1**), Λ-$[Co(H_2L)][Sb_2\{(R,R)\text{-tart}\}_2]$·$4H_2O$ (**2**), Λ-[Co(L)] (Λ-**3**), and H_3L.

Complex (Solvent)	UV/Vis λ [nm]	UV/Vis $\log\varepsilon$ [$M^{-1}cm^{-1}$]	CD λ [nm]	CD $\Delta\varepsilon$ [$M^{-1}cm^{-1}$]
Λ-**1** (dmso)	480^{sh}	2.41	488	–7.74
	320^{sh}	3.70	358	+18.0
	273	4.36	299	+28.4
			271	–38.5
2 (H_2O)	480^{sh}	2.34	487	–8.14
	320^{sh}	3.54	343	+17.4
	265	4.29	295	+32.2
			267	–46.0
Λ-**3** (MeOH)	480	2.35	481	–13.7
			340	46.7
H_3L (MeOH)	315^{sh}	3.19		
	255	4.58		

[sen = 1,1,1-tris(2′-aminoethylaminomethyl)ethane; $CH_3C(CH_2NHCH_2CH_2NH_2)_3$][8] than that of $[Co(en)_3]^{3+}$; therefore, the CD spectrum of Λ-**1** was compared with that of Λ-$[Co(sen)]^{3+}$. Λ-$[Co(sen)]^{3+}$ shows a small positive (λ = 503 nm, $\Delta\varepsilon$ = +0.42 $M^{-1}cm^{-1}$) and a relatively large negative CD band (λ = 450 nm, $\Delta\varepsilon$ = –1.05 $M^{-1}cm^{-1}$) in the first d–d absorption band region;[8] the positive CD component is diminished upon formation of a tripodal structure. This trend applies to Λ-**1**, where the positive CD band disappears completely. Λ-**1** also exhibits a positive CD band in the UV region at the longer wavelength side (λ = 358 nm, $\Delta\varepsilon$ = +18.0 $M^{-1}cm^{-1}$) of the imine (Schiff base) π–π* transition and a positive–negative couplet from longer to shorter wavelength in the 250–300 nm region. Exciton theory has been applied to tris(chelate)- or *cis*-bis(chelate)-type metal complexes containing chelate ligands such as 2,2′-bipyridine, 1,10-phenanthroline, or Schiff bases, and the relationship between the CD spectral pattern in the ligand π–π* transition region and the absolute configuration around the metal ion has been established.[9] A complex with a Λ configuration exhibits a positive–negative CD couplet from longer to shorter wavelength in the ligand π–π* transition. The assignment based on exciton theory agrees with the X-ray result (see below).

The uncoordinated NH groups of the imidazole moieties of **1** can be deprotonated by treatment with a base. We therefore performed a potentiometric pH titration of **1** in water and found the pK_1, pK_2, and pK_3 values to be 5.9, 7.2, and 8.5, respectively.[4a] We could not measure the pH-dependent electronic spectra of an aqueous solution of Λ-**1** due to the precipitation encountered during the titration procedure, therefore we carried out the measurements in methanol. Thus, aliquots of a methanolic $NaOCH_3$ solu-

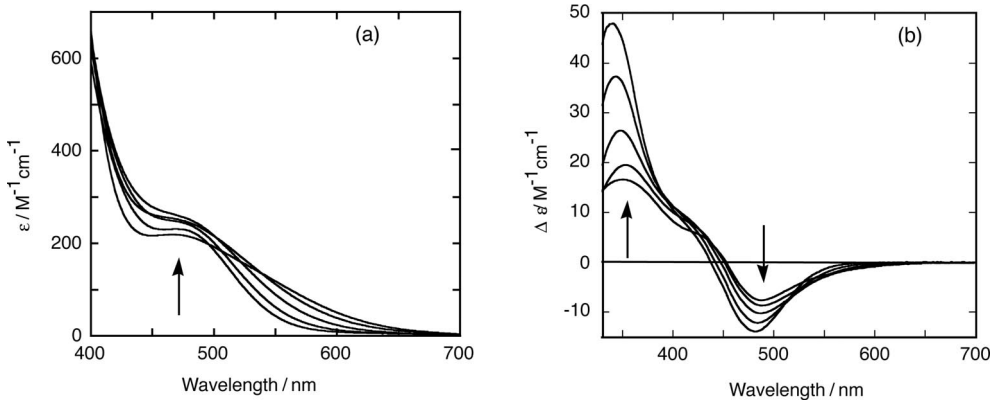

Figure 3. (a) UV/Vis and (b) CD spectral changes of Λ-$[Co(H_3L)](ClO_4)_3$·$1.5H_2O$ (Λ-**1**) upon the stepwise addition of $NaOCH_3$ in methanol (up to 3.0 equiv.; 0.0, 0.75, 1.5 , 2.25, and 3.0 equiv.) to a methanol solution of Λ-**1**.

tion (up to 3 equiv.) were added to Λ-$[Co(H_3L)]^{3+}$ in methanol, and the reaction was monitored by electronic and CD spectroscopy (Figure 3). Isosbestic points were not observed because many species {$[Co(H_3L)]^{3+}$, $[Co(H_2L)]^{2+}$, $[Co(HL)]^{+}$, and $[Co(L)]$} exist in equilibrium [Equation (1)].

$$[Co(H_3L)]^{3+} \underset{-H^+}{\overset{+H^+}{\leftrightarrows}} [Co(H_2L)]^{2+} \underset{-H^+}{\overset{+H^+}{\leftrightarrows}} [Co(HL)]^{+} \underset{-H^+}{\overset{+H^+}{\leftrightarrows}} [Co(L)] \quad (1)$$

The CD band maximum of the first d–d absorption band shifts to a shorter wavelength upon addition of the base, which suggests an increase in the ligand-field strength on deprotonation. These results are in agreement with our observations for related iron(II) and iron(III) complexes.[2] For example, the solution magnetic susceptibility measurements of $[Fe^{III}(H_3L)]^{3+}$ and $[Fe^{III}(L)]$ in CD_3OD at 297 K revealed that the former is in the high-spin state, while the latter is in the low-spin state with a larger ligand-field strength.[2] Although the UV/Vis spectral change upon deprotonation is not simple, the deprotonation–reprotonation reaction is reversible: protonation of [Co(L)] in methanol takes place upon sequential addition of HCl in methanol, and the complex is finally converted to $[Co(H_3L)]^{3+}$ (Figure S1 in the Supporting Information).

The electrochemical properties of $[Co(H_3L)]^{3+}$ (**1**) and its deprotonated forms were studied by cyclic voltammetry (CV). The measurements were performed under nitrogen with a glassy carbon working electrode using a methanol solution containing $LiClO_4$ (0.1 M) as supporting electrolyte. Complex **1** shows a quasi-reversible one-electron redox process ($Co^{III/II}$). The peak separation (ΔE_p) is larger than that expected for the reversible process (approx. 60 mV), and becomes larger as the scan rate (v) increases (Figure 4a): ΔE_p = 148 mV (E_{pc} = –0.498, E_{pa} = –0.350 V vs. Ag/Ag^+) at v = 20 mV s^{-1}; ΔE_p = 176 mV (E_{pc} = –0.503, E_{pa} = –0.327 V) at v = 50 mV s^{-1}; ΔE_p = 190 mV (E_{pc} = –0.507, E_{pa} = –0.317 V) at v = 100 mV s^{-1}; ΔE_p = 234 mV (E_{pc} = –0.514, E_{pa} = –0.280 V) at v = 200 mV s^{-1}. The analogous Fe and Ru complexes show electrochemically reversible $M^{III/II}$ (M = Fe, Ru) one-electron redox processes under the same conditions.[2,10] $[Co(H_3L)]^{3+}$ undergoes reversible deprotonation and protonation in methanol upon addition of a base and an acid, respectively, as described above. Figures 4b–d show the progress of the deprotonation–reprotonation reaction as monitored by CV (v = 100 mV s^{-1}). Addition of 1 equiv. of $NaOCH_3$ to a solution of $[Co(H_3L)]^{3+}$ in methanol causes the redox couple to shift to a more negative potential (E_{pc} = –0.56, E_{pa} = –0.42 V; Figure 4c), thereby showing that the compound becomes harder to reduce as the imidazole NH group is deprotonated. Carina et al.[11] have reported that deprotonation of the uncoordinated NH groups of the imidazole moieties switches the redox potential of an iron complex by as much as 345 mV per proton. It should be noted that the current intensity diminishes appreciably, and addition of a further 1 equiv. of $NaOCH_3$ (Figure 4d) causes the redox couple to disappear completely. Such a phenomenon was not observed for the Fe and Ru complexes, although the redox couples also shifted to a more negative value upon deprotonation.[2,10] Full deprotonation of the imidazolate nitrogen moieties is achieved by adding 3 equiv. of base to produce [Co(L)]. When 3 equiv. of HCl in MeOH was added to [Co(L)], the initial CV response for $[Co(H_3L)]^{3+}$ reappeared (Figure 4e). Thus, the deprotonation–protonation is reversible, as suggested by the UV/Vis and CD spectra. The reason why the $Co^{III/II}$ redox couple could not be observed after the addition of 2 or more equiv. of base to $[Co(H_3L)]^{3+}$ may be due to an overlap with other redox processes.

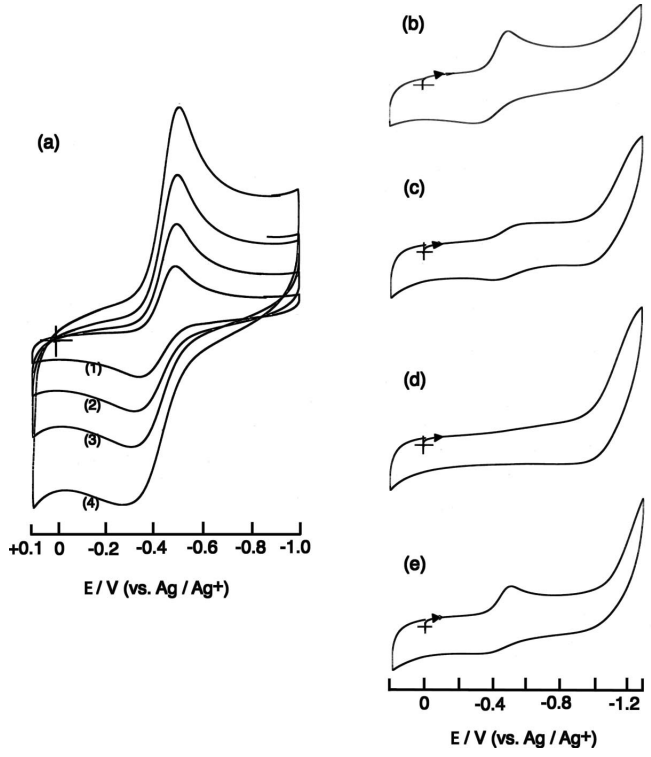

Figure 4. Cyclic voltammograms of $[Co(H_3L)](ClO_4)_3 \cdot H_2O$ (**1**; 0.2 mM) in methanol containing 0.1 M $LiClO_4$ at a glassy carbon electrode. (a) CV changes as a function of the sweep rate: (1) 20, (2) 50, (3) 100, (4) 200 mV s^{-1}. (b)–(e) show the progress of the deprotonation–reprotonation reaction as monitored by CV (v = 100 mV s^{-1}). (b) Before addition of $NaOCH_3$ in methanol. (c) Upon addition of 1 equiv. of $NaOCH_3$, the redox couple shifts to a more negative potential. (d) Upon addition of a further 1 equiv. (2 equiv. in total) of $NaOCH_3$, the redox couple disappears completely. (e) The initial CV response for $[Co(H_3L)]^{3+}$ reappears after adding 3 equiv. of HCl in MeOH to the fully deprotonated complex [Co(L)], which was achieved by adding 3 equiv. of base.

X-ray Crystal Structures

The crystal data and details of the structural determination for **1**, Λ-**1**, **2**, and Λ-**3** are summarized in Table 2. Although the ligand H_3L is potentially heptadentate, the tertiary amine nitrogen atom is not coordinated to the metal atom – the N(tertiary amine)···Co distance being 3.4–3.5 Å –, and the ligand is only hexadentate. Three imine (Schiff base) nitrogen atoms and three imidazole nitrogen atoms are coordinated in each complex to form an octahe-

Table 2. X-ray crystallographic data for $[Co(H_3L)](ClO_4)_3 \cdot H_2O$ (**1**), Λ-$[Co(H_3L)](ClO_4)_3 \cdot 1.5H_2O$ (Λ-**1**), Λ-$[Co(H_2L)][Sb_2\{(R,R)\text{-tart}\}_2] \cdot 4H_2O$ (**2**), and Λ-[Co(L)] (Λ-**3**).

	1	Λ-**1**	**2**	Λ-**3**
Empirical formula	$C_{18}H_{26}Cl_3CoN_{10}O_{13}$	$C_{18}H_{27}Cl_3CoN_{10}O_{13.5}$	$C_{26}H_{35}CoN_{10}O_{16}Sb_2$	$C_{18}H_{21}CoN_{10}$
Formula mass	755.75	764.76	1046.05	436.36
Crystal system	monoclinic	orthorhombic	orthorhombic	orthorhombic
Space group	$P2_1/a$ (no.14)	$P2_12_12_1$ (no.19)	$P2_12_12$ (no.18)	$P2_12_12_1$ (no.19)
a [Å]	12.7952(7)	12.4299(3)	12.7983(3)	9.831(2)
b [Å]	13.1764(5)	13.0278(3)	29.1216(7)	10.001(2)
c [Å]	17.9163(6)	36.4127(8)	9.4499(2)	19.699(4)
α [°]	90	90	90	90
β [°]	105.868(2)	90	90	90
γ [°]	90	90	90	90
V [Å^3]	2905.5(2)	5896.5(2)	3522.04(14)	1936.7(7)
Z	4	8	4	4
$D_{calcd.}$ [g cm^{-3}]	1.728	1.723	1.973	1.496
μ [cm^{-1}]	9.477	9.362	20.748	9.146
R_1[a] [$I > 2\sigma(I)$]	0.0386	0.0682	0.0576	0.0314
wR_2[b] [all data]	0.0997	0.1814	0.1610	0.0559
T [°C]	–50	–50	–50	20
Flack parameter		0.009(19)	0.03(2)	0.000(11)

[a] $R_1 = \Sigma(||F_o| - |F_c||)/\Sigma|F_o|$. [b] $wR_2 = [\Sigma\{w(F_o^2 - F_c^2)^2\}/\Sigma w(F_o^2)^2]^{1/2}$.

dral Co^{III} complex. The relevant coordination bond lengths for **1**, Λ-**1**, **2**, and Λ-**3** are listed in Table 3. The Co–N(imine) bond lengths are in the range 1.951–1.991 Å, while those for Co–N(imidazole) are in the range 1.899–1.928 Å. We have previously determined the X-ray crystal structures of the spin-crossover Fe^{II} complex $[Fe^{II}(H_3L)](BF_4)_2 \cdot 3H_2O$ at 293 and 108 K.[2] At 108 K, the complex is in the low-spin state and assumes a t_{2g}^6 electronic configuration, as does the Co^{III} compound **1**. However, the Fe–N(imine) [1.989(4) Å] and the Fe–N(imidazole) bond lengths [1.981(3) Å] in the Fe^{II} complex are almost the same, whereas the Ru–N(imine) bond length (av. 2.172 Å) in $[Ru^{II}(H_3L)](ClO_4)_2 \cdot 3H_2O$ ($4d^6$, t_{2g}^6), is apparently smaller than the Ru–N(imidazole) distance (av. 2.204 Å).[10] These results may indicate a difference in the nature of the bonding between the complexes. Each complex is chiral with either the Δ (clockwise) or Λ (anticlockwise) configuration due to the screw coordination arrangement of the tripodal ligand around the Co^{III} ion. The absolute configurations of the chiral crystals that were subjected to X-ray analyses were determined from their Flack parameters.[12]

Table 3. Coordination bond lengths [Å] for $[Co(H_3L)](ClO_4)_3 \cdot H_2O$ (**1**), Λ-$[Co(H_3L)](ClO_4)_3 \cdot 1.5H_2O$ (Λ-**1**), Λ-$[Co(H_2L)][Sb_2\{(R,R)\text{-tart}\}_2] \cdot 4H_2O$ (**2**), and Λ-[Co(L)] (Λ-**3**).

	1	Λ-**1**	**2**	Λ-**3**
Co(1)–N(2)	1.958(2)	1.951(4)	1.966(5)	1.9546(17)
Co(2)–N(12)		1.964(5)		
Co(1)–N(3)	1.918(2)	1.927(5)	1.910(5)	1.8988(18)
Co(2)–N(13)		1.923(5)		
Co(1)–N(5)	1.961(2)	1.991(4)	1.961(5)	1.9577(16)
Co(2)–N(15)		1.971(5)		
Co(1)–N(6)	1.910(2)	1.919(4)	1.920(5)	1.9041(18)
Co(2)–N(16)		1.926(5)		
Co(1)–N(8)	1.964(2)	1.963(5)	1.962(5)	1.9587(18)
Co(2)–N(18)		1.958(5)		
Co(1)–N(9)	1.908(2)	1.928(5)	1.912(5)	1.8991(18)
Co(2)–N(19)		1.901(5)		

Structure of $[Co(H_3L)](ClO_4)_3 \cdot H_2O$ (1)

Crystals of **1** suitable for an X-ray crystal structure analysis were grown in a refrigerator. Complex **1** crystallizes in the space group $P2_1/a$ (no. 14) with $Z = 4$. In a previous paper,[4a] we reported that the same complex crystallizes at room temperature in the space group Cc (no. 9) with $Z = 8$, although the crystal structure is almost the same as that of the present complex ($P2_1/a$).

Figure 5 shows an ORTEP drawing of the $[Co(H_3L)]^{3+}$ cation of **1** with the Λ absolute configuration. Molecules with the Δ and the Λ absolute configurations coexist in the crystal to form a racemate. Figure 6 shows a packing diagram in which dark gray and light gray molecules represent

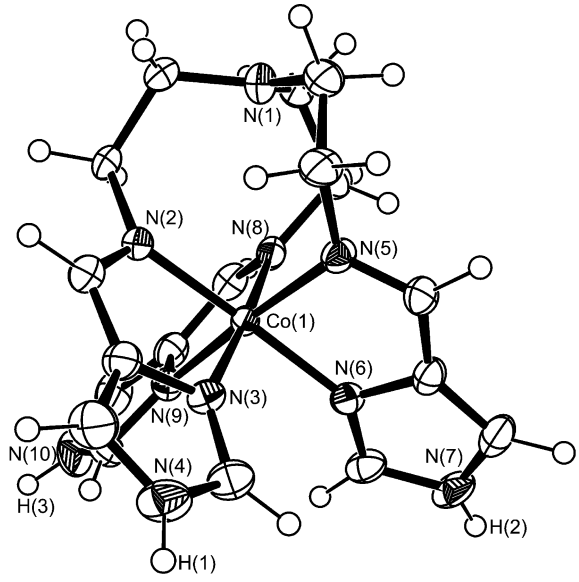

Figure 5. X-ray molecular structure of the cation of $[Co(H_3L)](ClO_4)_3 \cdot H_2O$ (**1**), with atomic numbering scheme, showing 50% probability ellipsoids. The complex shown here has the Λ absolute configuration.

the Λ and the Δ enantiomers, respectively. Each [Co(H$_3$L)]$^{3+}$ cation is connected to one water molecule and two ClO_4^- anions by hydrogen bonds [N(4)–H(7)···O(13) 2.785(5), N(7)–H(15)···O(1) 2.941(3), N(10)–H(23)···O(5) 2.927(3), N(10)–H(23)···O(6) 3.036(3) Å]. No hydrogen bond is observed between these hydrogen-bonded clusters. This situation is almost the same as that of the crystal having the space group of *Cc*, with the only difference between the two structures being the orientation of the ClO_4^- anion not involved in hydrogen bonding (Figure S2 in the Supporting Information).

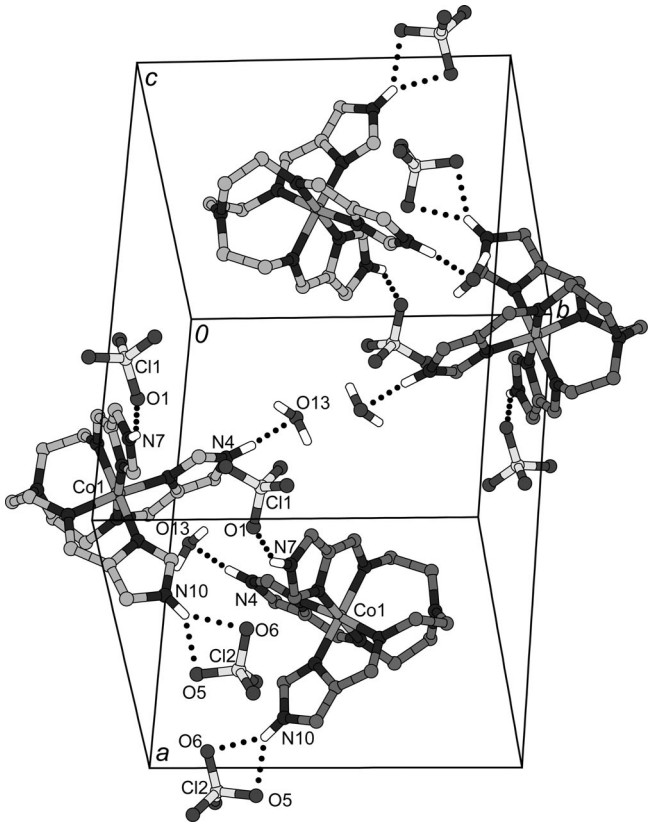

Figure 6. Crystal structure of [Co(H$_3$L)](ClO$_4$)$_3$·H$_2$O (**1**). The dark gray and light gray molecules represent the Λ and the Δ enantiomers, respectively. Each [Co(H$_3$L)]$^{3+}$ cation is connected to one water molecule and two ClO_4^- anions by hydrogen bonds. No hydrogen bond is observed between these hydrogen-bonded clusters. Hydrogen atoms on carbon atoms and ClO_4^- anions not involved in hydrogen bonding have been omitted for clarity.

Structure of Λ-[Co(H$_3$L)](ClO$_4$)$_3$·1.5H$_2$O (Λ-1)

Optically active Λ-**1** crystallizes in the orthorhombic space group $P2_12_12_1$ (no. 19) with $Z = 8$. Its crystal structure (Figure 7) consists of two [Co(H$_3$L)]$^{3+}$ cations, six ClO_4^- anions, and three water molecules as the asymmetric unit. The two complex cations, one ClO_4^- anion and one water molecule are connected by hydrogen bonds to form a 1D network structure running along the [$\bar{1}$10] direction [Figure 7(a); O(19)···N(7) 2.881(9), N(4)···O(28) 3.037(9), O(28)···N(20) 2.797(8), N(17)···O(18) 2.906(9) Å]. N(4) is also connected to ClO_4^- [N(4)···O(8) 3.013(8) Å]. A symmetry operation also produces the same 1D structure running along the [110] direction [Figure 7(b)]. The remaining uncoordinated imidazole NH groups are also connected to a ClO_4^- anion or a water molecule by hydrogen bonds {N(10)···O(26) 3.182(16), N(10)···O(27) 2.85(2) [both O(26) and O(27) are disordered with an occupancy of 1/2], and N(14)···O(29) 2.787(10) Å}. No interchain hydrogen bonds are observed. The average coordinate bond lengths [Co–N(imine) 1.966, Co–N(imidazole) 1.921 Å] and the average N(imidazole)–Co–N(imidazole) angle (93.4°) are similar to those of the racemic complex **1** [Co–N(imine) 1.961, Co–N(imidazole) 1.912 Å; N(imidazole)–Co–N(imidazole) 93.01°].

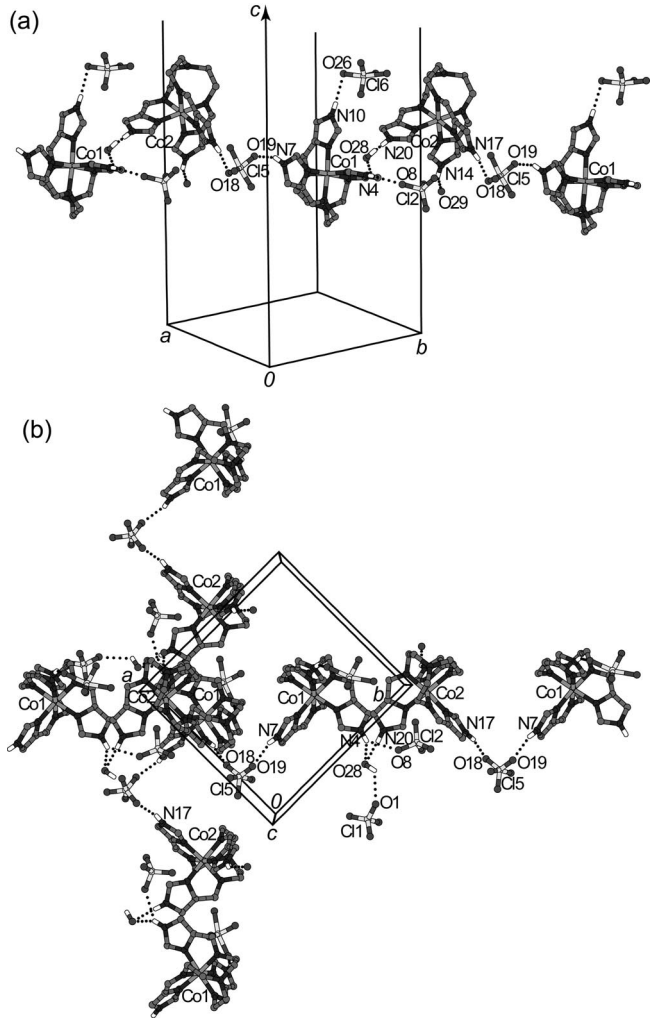

Figure 7. Extended intermolecular structure of Λ-[Co(H$_3$L)](ClO$_4$)$_3$·1.5H$_2$O (Λ-**1**). (a) Two complex cations, one ClO_4^- anion, and one water molecule are connected by hydrogen bonds to form a 1D network structure running along the [$\bar{1}$10] direction. (b) A 1D structure running along the [110] direction produced by a symmetry operation.

Structure of Λ-[Co(H$_2$L)][Sb$_2${(R,R)-tart}$_2$]·4H$_2$O (2)

Figure 8 shows the crystal structure of **2**, which crystallizes in the space group $P2_12_12$ (no. 18) with $Z = 4$. The crystal structure consists of one $[Co(H_2L)]^{2+}$ dication, two half $[Sb_2\{(R,R)\text{-tart}\}_2]^{2-}$ dianions, and four water molecules (three molecules with an occupancy of 1 and two with an occupancy of 1/2) in the asymmetric unit. One of the three uncoordinated imidazole NH groups of the tripodal ligand is deprotonated, and the complex cation is formulated as $[Co(H_2L)]^{2+}$. The presence or absence of NH protons was determined from the electron density map. The X-ray structures of quite a few metal complexes with the neutral H_3L ligand and its derivatives, as well as several with the fully deprotonated ligand (L^{3-}), have been reported.[2–4,10,13,14] It should be noted that a formally hemi-deprotonated species, for example $[Co^{III}(H_{1.5}L)]^{1.5+}$, consists of a complex with the ligand in the neutral form $\{[Co^{III}(H_3L)]^{3+}\}$ and a complex with the fully deprotonated ligand $\{[Co^{III}(L)]^0\}$, and thus a more appropriate formulation would be $[\{Co^{III}(H_3L)\}\{Co^{III}(L)\}]^{3+}$. Except for $[Fe^{III}(HL^{Me})]^+$,[13f] the NH moiety of which suffers from disorder, **2** is the first complex with a partially deprotonated imine–imidazole ligand. In general, the Co–N(imidazolate) bond is shorter than the Co–N(imidazole) bond.[4] This applies to complex **2**, although the difference is not large. The Co–N(imidazolate) bond, [Co(1)–N(3) 1.910(5) Å] is shorter than the Co–N(imidazole) bonds, [Co(1)–N(6) 1.920(5), Co(1)–N(9) 1.912(5) Å].

Adjacent complex cations with the Λ absolute configuration are connected in a tail-to-tail fashion by N(4)···H(22)–N(10) hydrogen bonds in the crystal of **2** to form a 1D zigzag chain structure along the *a* axis [N(4)···N(10) 2.701(9) Å; Figure 8(b)]. The remaining uncoordinated imidazole N(7)–H(14) group is hydrogen-bonded to the O(1) and O(11) atoms of the $[Sb_2\{(R,R)\text{-tart}\}_2]^{2-}$ dianion [N(7)···O(1) 3.045(8), N(7)···O(11) 2.934(9) Å]. Thus, the 1D zigzag chains are connected by N(7)···O(1) and

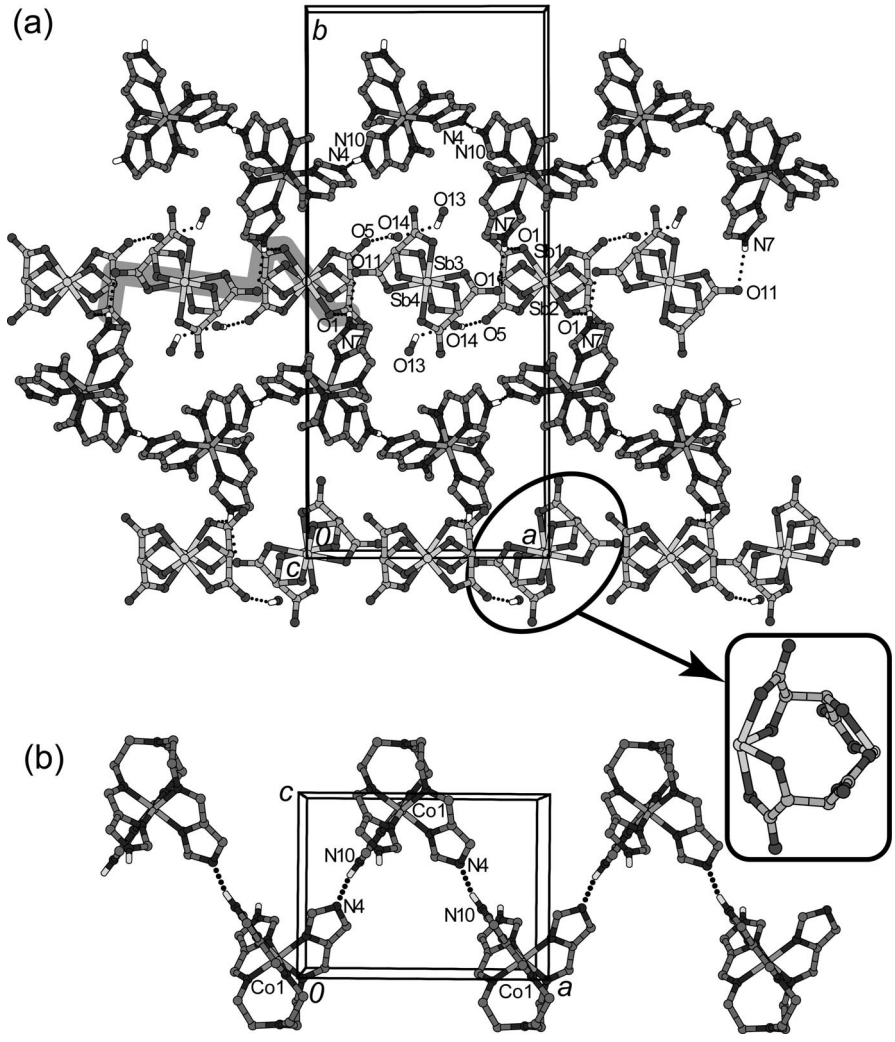

Figure 8. Crystal structure of Λ-[Co(H$_2$L)][Sb$_2${(*R*,*R*)-tart}$_2$]·4H$_2$O (**2**). The carbon atoms of Λ-$[Co(H_2L)]^{2+}$ and $[Sb_2\{(R,R)\text{-tart}\}_2]^{2-}$ are shown in dark gray and light gray, respectively. (a) Top view. Adjacent complex cations are connected by N(4)···H(22)–N(10) hydrogen bonds to form a 1D zigzag chain structure along the *a*-axis. These 1D chains are connected by the N(7)···O(1) and N(7)···O(11) hydrogen bonds shown by the wide gray line to form a 2D sheet structure. (b) Side view showing a zigzag chain structure.

N(7)···O(11) hydrogen bonds [thick gray line in Figure 8(a)] to form a 2D sheet structure. These sheets are stacked along the *c* axis.

A perspective view of the $[Sb_2\{(R,R)\text{-tart}\}_2]^{2-}$ dianion is also given in Figure 8(a). The dimeric structure is built up of two tetradentate tartrate ions and two antimony atoms. The coordination geometry around each Sb atom can be described as ψ-trigonal-bipyramidal. A lone pair of electrons seems to occupy one of the equatorial positions, and the alkoxide oxygen atoms reside in the remaining equatorial positions with metal–oxygen distances of 1.964(3)–1.987(3) Å. Two carboxylate oxygen atoms occupy the apical positions, with metal–oxygen distances of 2.160(3)–2.177(3) Å. These structural features are quite similar to those of the anion of $K_2[Sb_2\{(R,R)\text{-tart}\}_2]\cdot 3H_2O$ and related compounds.[15]

Structures of rac-[Co(L)]·2.5H_2O (3) and Λ-[Co(L)] (Λ-3)

The fully deprotonated racemic complex *rac*-[Co(L)]·2.5H_2O (**3**) contains water molecules of crystallization. We have already reported the crystal structure of **3**,[4a] which crystallizes in the cubic space group $I\bar{4}3d$ with $Z = 16$. The crystal structure consists of one [Co(L)] unit and 2.5 water molecules. The uncoordinated imidazole nitrogen atoms are hydrogen-bonded to water molecules, and the neighboring water molecules are further hydrogen-bonded to each other to form an extended intermolecular network structure. It should be noted that the complex molecules with the same absolute configuration are connected by hydrogen bonding [Figure 9(a)]. However, a detailed network structure cannot be described owing to disorder of the water molecules.

Complex Λ-**3** crystallizes in the orthorhombic non-centrosymmetric space group $P2_12_12_1$ with $Z = 4$. There is no water of crystallization, and the crystal structure consists of only one [Co(L)] moiety as the asymmetric unit [Figure 9(b)]. The complex molecules interact with each other through two kinds of CH–π stacking [C6–H7···N9–C16–C18–N10–C17 (imidazole ring of a neighboring molecule) and C12–H14···N3–C4–C6–N4–C5 (ring of another neighboring molecule) with H to ring distances of 2.736 and 2.979 Å, respectively] and a C(18)–H(21)···N(7)* hydrogen bond [C(18)···N(7)* 3.563(3) Å] to form a 3D network. The average bond lengths in Λ-**3** [Co–N(imine) 1.9570, Co–N(imidazole) 1.9007 Å] and the average N(imidazole)–Co–N(imidazole) bond angle (82.56°) are close to those of the racemic complex **3** [Co–N(imine) 1.955(5), Co–N(imidazole) 1.911(5) Å; N(imidazole)–Co–N(imidazole) 80.8(2)°].[4a]

Concluding Remarks

Optical resolution of $[Co(H_2L)]^{2+}$, which is a mono-deprotonated derivative of $[Co(H_3L)]^{3+}$, has been carried out by fractional crystallization of the diastereomeric salt with $[Sb_2\{(R,R)\text{-tart}\}_2]^{2-}$. The X-ray crystal structure analysis of the less soluble diastereomer, $\{(-)_{487}\}_{CD}$-Λ-$[Co(H_2L)]$-$[Sb_2\{(R,R)\text{-tart}\}_2]\cdot 4H_2O$ (**2**), reveals that each complex cation is connected to an adjacent complex cation and $[Sb_2\{(R,R)\text{-tart}\}_2]^{2-}$ by hydrogen bonds to form a 2D sheet structure. The formation of a well-developed hydrogen-bonding network may be responsible for the crystallization of **2**. The other diastereomer, Δ-$[Co(H_2L)][Sb_2\{(R,R)\text{-tart}\}_2]$, seems to be much more soluble, and all efforts to isolate it were unsuccessful. The structures of the perchlorate salt (Λ-**1**) derived from **2** and the racemic analog **1** have been compared. Λ-**1** has an extended 1D intermolecular network structure, while **1** does not. Complex **1** and the analogous ruthenium(II) complex $[Ru(H_3L)](ClO_4)_2$ do not undergo conglomerate crystallization, whereas the corresponding iron(II) complex $[Fe(H_3L)](ClO_4)_2\cdot 3H_2O$ un-

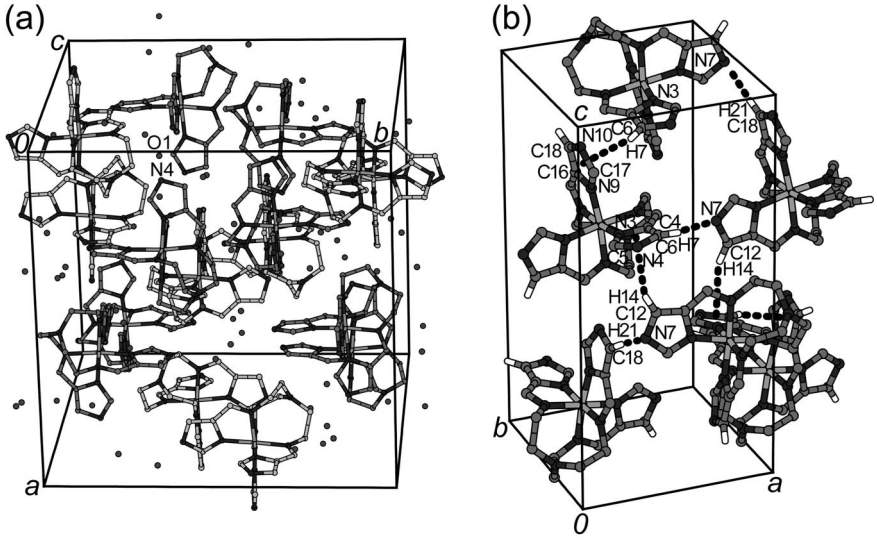

Figure 9. Crystal structures of fully deprotonated species. (a) Crystal structure of [Co(L)]·2.5H_2O (**3**). The light gray and dark gray molecules represent the Δ and the Λ enantiomer, respectively (see text for further details). (b) Crystal structure of Λ-[Co(L)] (Λ-**3**). Complex molecules interact with each other with two kinds of CH–π stacking and a CH···N hydrogen bond (see text).

dergoes homochiral crystallization to form a conglomerate. The water molecules of crystallization and the charge of the complex seem to be the main factors influencing conglomerate crystallization, although this problem needs to be discussed further.

Experimental Section

Caution! Perchlorate salts of metal complexes are potentially explosive. Only small quantities of material should be prepared, and the samples should be handled with care.

Materials: All reagents and solvents in the syntheses were of reagent grade and used without further purification. $[Co(H_3L)](ClO_4)_3 \cdot H_2O$ (**1**) and $[Co(L)] \cdot 2.5H_2O$ (**3**) were prepared according to a literature procedure.[4a]

Λ-$[Co(H_2L)][Sb_2\{(R,R)\text{-tart}\}_2] \cdot 4H_2O$ (2): An aqueous solution of $[Co(H_3L)](ClO_4)_3 \cdot H_2O$ (3.68 g, 5.0 mmol) was stirred with an anion exchange resin (Dowex 1X8 in the Cl^- form), and then the whole suspension was poured onto a column (1.0 cm i.d. × 15 cm) of the same exchange resin to ensure conversion into the chloride. The column was washed with water, and the effluent containing $[Co(H_3L)]Cl_3$ (5.0 mmol) was mixed with a suspension of $Ag_2[Sb_2\{(R,R)\text{-tart}\}_2]$[16] (3.76 g, 5.0 mmol) and $NaHCO_3$ (0.42 g, 5.0 mmol) in water. The mixture was stirred in the dark for 1 h, and then filtered through Celite to remove AgCl. The filtrate was concentrated in a rotary evaporator to give a reddish orange precipitate, which was repeatedly recrystallized from water until the CD intensity had become constant. Yield: 1.79 g (35%). $C_{26}H_{35}CoN_{10}O_{16}Sb_2$ (1046.11): calcd. C 29.85, H 3.37, N 13.39; found C 29.61, H 3.23, N 13.20.

Λ-$[Co(H_3L)](ClO_4)_3 \cdot 1.5H_2O$ (Λ-1): The diastereomer Λ-$[Co(H_2L)][Sb_2\{(R,R)\text{-tart}\}_2] \cdot 4H_2O$ (**2**; 1.05 g, 1.0 mmol) was converted into its chloride with Dowex 1X8 (Cl^- form), as described for the conversion of $[Co(H_3L)](ClO_4)_3 \cdot H_2O$ into its chloride salt. An aqueous solution of Λ-$[Co(H_3L)]Cl_3$ (1.0 mmol) was mixed with $AgClO_4$ (0.622 g, 3.0 mmol) and the mixture stirred for 1 h. AgCl was removed by filtration, and the filtrate concentrated to give dark red crystals. Yield: 0.71 g (92%). $C_{18}H_{27}Cl_3CoN_{10}O_{13.5}$ (764.76): calcd. C 28.27, H 3.56, N 18.32; found C 28.14, H 3.40, N 18.07. IR (KBr disk): $\nu_{C=N}$(imine): 1626; ν_{Cl-O}(ClO_4^-): 1142, 1117, 1088 cm^{-1}.

Λ-[Co(L)] (Λ-3): The diastereomer Λ-$[Co(H_2L)][Sb_2\{(R,R)\text{-tart}\}_2] \cdot 4H_2O$ (**2**; 0.32 g, 0.3 mmol) was converted into its chloride by the method described for the synthesis of Λ-**1**. Addition of 1.0 M NaOH (3.0 mL, 3.0 mmol) to an aqueous solution of Λ-$[Co(H_3L)]Cl_3$ (0.3 mmol) and concentration of the mixture in a rotary evaporator gave orange crystals, which were recrystallized from water/methanol. Yield: 0.10 g (77%). $C_{18}H_{21}CoN_{10}$ (436.36): calcd. C 49.54, H 4.85, N 32.10; found C 49.28, H 4.63, N 31.74. IR (KBr disk): $\nu_{C=N}$(imine): 1590 cm^{-1}.

Physical Measurements: UV/Vis spectra were recorded with a JASCO Ubest-550 spectrophotometer. Infrared spectra were recorded with a JASCO FT/IR-550 spectrophotometer. CD spectra were recorded with a JASCO J-720 spectropolarimeter. CV measurements were performed under nitrogen using a Fuso HECS 321B potential sweep unit with methanol solutions containing $LiClO_4$ (0.1 M) as supporting electrolyte. The electrochemical cell was a three-electrode system consisting of a glassy carbon working electrode, a platinum wire auxiliary electrode, and an Ag/Ag^+ (Ag/0.01 M $AgNO_3$) reference electrode. The couple of the external standard (Fc/Fc^+; Fc = ferrocene) was observed at –0.170 V vs. Ag/Ag^+ under the same conditions.

X-ray Data Collection, Reduction, and Structure Determination: X-ray data were collected with a Rigaku R-AXIS RAPID II imaging-plate area detector using graphite-monochromated Mo-K_α radiation (λ = 0.71073 Å). The structures were solved by direct methods, and refined using full-matrix least-squares procedures with the CrystalStructure crystallographic software package.[17] The absolute configuration was determined on the basis of the Flack parameters.[12] CCDC-660017 (**1**), -660018 (Λ-**1**), -660019 (**2**), and -660020 (Λ-**3**) contain the supplementary crystallographic data for this paper. These data can be obtained free of charge from The Cambridge Crystallographic Data Center via www.ccdc.cam.ac.uk/data_request/cif.

Supporting Information (see footnote on the first page of this article): UV/Vis and CD spectral changes of Λ-[Co(L)] upon sequential addition of HCl in methanol and comparison of the two crystal structures of $[Co(H_3L)](ClO_4)_3 \cdot H_2O$ [**1**; $P2_1/c$ and Cc].

Acknowledgments

This work was supported in part by a Grant-in-Aid for Scientific Research from the Ministry of Education, Science, Sports, and Culture of Japan (grant nos. 16205010, 16750050, and 17350028) and by the Iketani Science and Technology Foundation.

[1] E. L. Eliel, S. H. Wilen, *Stereochemistry of Organic Compounds*, Wiley, New York, **1994**.
[2] Y. Sunatsuki, H. Ohta, M. Kojima, Y. Ikuta, Y. Goto, N. Matsumoto, S. Iijima, H. Akashi, S. Kaizaki, F. Dahan, J.-P. Tuchagues, *Inorg. Chem.* **2004**, *43*, 4154–4171.
[3] a) H. Ohta, Y. Sunatsuki, Y. Ikuta, N. Matsumoto, S. Iijima, H. Akashi, T. Kambe, M. Kojima, *Mater. Sci.* **2003**, *21*, 191–198; b) Y. Sunatsuki, Y. Ikuta, N. Matsumoto, H. Ohta, M. Kojima, S. Iijima, S. Hayami, Y. Maeda, S. Kaizaki, F. Dahan, J.-P. Tuchagues, *Angew. Chem. Int. Ed.* **2003**, *42*, 1614–1618; c) H. Ohta, Doctoral Dissertation, Okayama University, Okayama, Japan, **2004**.
[4] a) I. Katsuki, Y. Motoda, Y. Sunatsuki, N. Matsumoto, T. Nakashima, M. Kojima, *J. Am. Chem. Soc.* **2002**, *124*, 629–640; b) H. Nakamura, Y. Sunatsuki, M. Kojima, N. Matsumoto, *Inorg. Chem.* **2007**, *46*, 8170–8181.
[5] A. Werner, R. Feenstra, *Ber. Dtsch. Chem. Ges.* **1906**, *39*, 1538.
[6] a) Y. Tanabe, S. Sugano, *J. Phys. Soc. Jpn.* **1954**, *9*, 753–766; b) A. B. P. Lever, *Inorganic Electronic Spectroscopy*, Elsevier, Amsterdam, **1968**.
[7] a) Y. Saito, K. Nakatsu, M. Shiro, H. Kuroya, *Bull. Chem. Soc. Jpn.* **1957**, *30*, 795–798; b) S. F. Mason, B. J. Peart, *J. Chem. Soc., Dalton Trans.* **1977**, 937–941; c) A. J. McCaffery, S. F. Mason, *Mol. Phys.* **1963**, *6*, 359–371; d) Y. Sato, *Inorganic Molecular Dissymmetry*, Springer-Verlag, Berlin, **1979**; e) S. F. Mason, *Molecular Optical Activity & the Chiral Discriminations*, Cambridge University Press, London, **1982**.
[8] J. E. Sarneski, F. L. Urbach, *J. Am. Chem. Soc.* **1971**, *93*, 884–888.
[9] a) B. Bosnich, A. T. Phillip, *J. Am. Chem. Soc.* **1968**, *90*, 6352–6359; b) J. Hidaka, B. E. Douglas, *Inorg. Chem.* **1964**, *3*, 1180–1184; c) J. W. Canary, C. S. Allen, *J. Am. Chem. Soc.* **1995**, *117*, 8484–8485; d) S. Zahn, J. W. Canary, *Angew. Chem. Int. Ed.* **1998**, *37*, 305–308; e) J. M. Castagnetto, J. W. Canary, *Chem. Commun.* **1998**, 203–204.
[10] T. Yamaguchi, K. Harada, Y. Sunatsuki, M. Kojima, K. Nakajima, N. Matsumoto, *Eur. J. Inorg. Chem.* **2006**, 3236–3243.
[11] R. F. Carina, R. F. Verzegnassi, G. Bernardinelli, A. F. Williams, *Chem. Commun.* **1998**, 2681–2682.
[12] H. D. Flack, *Acta Crystallogr., Sect. A* **1993**, *39*, 876–881.

[13] a) C. Brewer, G. Brewer, C. Luckett, G. S. Marbury, A. M. Beatty, W. R. Scheidt, *Inorg. Chem.* **2004**, *43*, 2402–2415; b) G. Brewer, C. Luckett, *Inorg. Chim. Acta* **2005**, *358*, 239–245; c) C. Brewer, G. Brewer, G. Patil, Y. Sun, C. Viragh, R. J. Butcher, *Inorg. Chim. Acta* **2005**, *358*, 3441–3448; d) C. Brewer, G. Brewer, R. J. Butcher, E. E. Carpenter, L. Cuenca, A. M. Schmiedekamp, C. Viragh, *Dalton Trans.* **2005**, 3617–3619; e) G. Brewer, C. Brewer, R. J. Butcher, E. E. Carpenter, *Inorg. Chim. Acta* **2006**, *359*, 1263–1268; f) C. Brewer, G. Brewer, R. J. Butcher, E. E. Carpenter, L. Cuenca, B. C. Noll, W. R. Scheidt, C. Viragh, P. Y. Zavalij, D. Zielaski, *Dalton Trans.* **2006**, 1009–1019; g) M. Mimura, T. Matsuo, Y. Motoda, N. Matsumoto, T. Nakashima, M. Kojima, *Chem. Lett.* **1998**, 691–692; h) I. Katsuki, N. Matsumoto, M. Kojima, *Inorg. Chem.* **2000**, *39*, 3350–3354; i) N. Matsumoto, I. Katsuki, Y. Motoda, M. Kojima, *Mol. Cryst. Liq. Cryst. Sci. Technol., Sect. A* **2000**, *342*, 177–184; j) S. Nagasato, I. Katsuki, Y. Motoda, Y. Sunatsuki, N. Matsumoto, M. Kojima, *Inorg. Chem.* **2001**, *40*, 2534–2540; k) Y. Sunatsuki, M. Sakata, S. Matsuzaki, N. Matsumoto, M. Kojima, *Chem. Lett.* **2001**, 1254–1255; l) M. Yamada, H. Hagiwara, H. Torigoe, N. Matsumoto, M. Kojima, F. Dahan, J.-P. Tuchagues, N. Re, S. Iijima, *Chem. Eur. J.* **2006**, *12*, 4536–4549; m) F. Lambert, C. Policar, S. Durot, M. Cesario, L. Yuwei, H. Korri-Youssoufi, B. Keita, L. Nadjo, *Inorg. Chem.* **2004**, *43*, 4178–4188; n) H. He, K. R. Rodgers, A. M. Arif, *J. Inorg. Biochem.* **2004**, *98*, 667–676.

[14] a) Y. Ikuta, M. Ooidemizu, Y. Yamahata, M. Yamada, S. Osa, N. Matsumoto, S. Iijima, Y. Sunatsuki, M. Kojima, F. Dahan, J.-P. Tuchagues, *Inorg. Chem.* **2003**, *42*, 7001–7017; b) M. Yamada, M. Ooidemizu, Y. Ikuta, S. Osa, N. Matsumoto, S. Iijima, M. Kojima, F. Dahan, J.-P. Tuchagues, *Inorg. Chem.* **2003**, *42*, 8406–8416.

[15] a) M. E. Gress, R. A. Jacobsen, *Inorg. Chim. Acta* **1974**, *8*, 209–217; b) R. E. Tapscott, R. L. Belford, I. C. Paul, *Coord. Chem. Rev.* **1969**, *4*, 323–359.

[16] T. J. Rutherford, P. A. Pellegrini, J. Aldrich-Wright, P. C. Junk, F. R. Keene, *Eur. J. Inorg. Chem.* **1998**, 1677–1688.

[17] *CrystalStructure 3.8*, Crystal Structure Analysis Package, Rigaku and Rigaku/MSC, The Woodlands, TX, USA, **2001**–**2006**.

Received: September 12, 2007
Published Online: January 15, 2008

